ELSEVIER

Thin Solid Films 267 (1995) 134–137

thin solid films

The epitaxial growth of IV–VI heterostructures and superlattices on (001)Si

A.I. Fedorenko [a], A.G. Fedorov [a], A.Yu. Sipatov [a], O.A. Mironov [b,*,1]

[a] *Kharkov State Polytechnic University, Kharkov, 310002, Ukraine*

[b] *Department of Physics, University of Warwick, Coventry CV4 7AL, UK*

Abstract

We report for the first time the use of rare-earth chalcogenides as buffer layers on silicon substrates prior to the high vacuum epitaxy of IV–VI compounds for the growth of thin film heterostructures and superlattices. The results of X-ray diffraction characterisation showed that YbS grows at 900–950 °C on (001) Si as a high-quality single crystal layer with an X-ray rocking curve half width $\delta = 300$–500 arcsec. Such buffer layers allow us to grow single-crystal IV–VI films and various types of heterostructures and superlattices with crystal quality better than that achievable in the buffer layer (with $\delta = 100$–300 arcsec), over a large area with good uniformity.

Keywords: Lead telluride; Silicon; Transmission electron microscopy; X-ray diffraction

1. Introduction

IV–VI narrow gap semiconductors are well known infrared (IR) materials. Their growth on Si substrates opens up a unique possibility for a new generation of integrated IR optoelectronic device fabrication: infrared sensor arrays (IRSA). Such IRSA were previously grown only when CaF_2–BaF_2 buffer layers were used [1], which are, however, not suitable for conventional wet photolithographic processing. Unfortunately, in the case of (001)Si substrates there are other kinds of problems with the stability of IV–VI films due to the fact that fluorides have a preferred (111) growth mode. We suggest rare-earth chalcogenides as alternative buffer layers for the high-vacuum epitaxial growth of IV–VI optoelectronic structures on (001)Si.

2. Experimental procedure

High-vacuum technology was developed for the reproducible deposition of lead, tin, europium and ytterbium chalcogenide heterostructures and superlattices, with layer thicknesses of between 1.0–100.0 nm. The samples were grown in an oil-free high vacuum system (residual pressure $P_{res} = 10^{-6}$ to 10^{-7} Pa) by thermal evaporation of lead chalcogenides (PbS, PbSe, PbTe) from boats and electron-beam evaporation of rare-earth chalcogenides (YbS, YbSe, YbTe, EuS, EuSe, and EuTe). Single-layer YbS films were deposited on (001) Si substrates at 900–950 °C. The substrates were heated by a quartz lamp with the temperature controlled using a thermocouple. Heterostructures and superlattices were grown by alternate deposition of two chalcogenides on silicon substrates. The layer thickness and deposition rate were monitored by a calibrated quartz resonator. Before loading into the vacuum chamber, substrates were prepared using standard cleaning in boiling solutions of $H_2O_2 + NH_4OH + H_2O$ and $H_2O_2 + HCL + H_2O$. Prior to film deposition the substrates were heated up to 950 °C over a period of 5 min at $P_{res} = 2 \times 10^{-7}$ Pa, for the removal of surface oxides. The film structure was studied by X-ray topography (XRT) and X-ray rocking curve (XRRC) measurements. X-ray diffraction (XRD) patterns of films and superlattices were obtained with the help of a double-crystal spectrometer using Cu Kα radiation. The (400) reflection from a Si monochromator and (200) reflection from the samples in (Θ–2Θ) arrangement were used. Lead chalcogenide films and heterostructures were also grown on (001)KCl substrates and were characterised by XRT and XRD for the comparison of their structural qualities with that of the IV–VI films grown on (001)Si substrates.

* Corresponding author. Fax: +44 (0)1203 69 20 16. E-mail: o.a.mironov@csv.warwick.ac.uk.

[1] On leave from Institute of Radiophysics and Electronics, National Academy of Sciences of Ukraine, Kharkov, 310085, Ukraine.

SSDI 0040-6090(95)06663-2

3. Results and discussion

3.1. Heterostructures

Preliminary investigations showed that lead chalcogenides grew on silicon substrates by an islanding mechanism (the Volmer–Weber mode), forming polycrystalline or textured films. We can explain such results in terms of the negligible influence of silicon substrate orientation, caused by weak bonding between the condensate and substrate and a too low substrate temperature. Better silicon orientation influence is obtained at higher temperatures (700–900 °C). However, an increase of the substrate temperature T_s above 400–450 °C for lead chalcogenides is impossible, because of the desorption of constituent species from the substrate. The use of more suitable refractory materials, with similar lattice parameters and chemical bonding properties to the IV–VI compounds, can result in both the layer-by-layer growth mechanism (the Frank–van der Merve mode) and crystalline perfection of the films. We select for this purpose the rare-earth chalcogenides (see Table 1) as more promising materials for buffer layers, instead of the familiar fluoride compounds CaF_2 and BaF_2 [1].

It is known that lead and rare-earth chalcogenides grow on top of each other in the layer-by-layer mode, with a high-quality crystalline structure [2,3]. Rare-earth chalcogenides are high-temperature melting materials and can grow on Si at the high temperatures necessary for epitaxial growth.

Structural investigations show that YbS grows on (001) Si substrates as polycrystalline films at low temperatures ($T_s < 400$ °C). Increasing the temperature up to 500–800 °C gives the [001] texture. But only at high temperatures (900–950 °C) does YbS grow as a monocrystalline film in the (001) orientation. The XRRC half-width of YbS films is $\delta = 300$–600 arcsec, comparable with the XRRC half-width of PbS films on (001) KCl ($\delta = 300$ arcsec).

Investigation of lead chalcogenide epitaxial growth at $T_s = 300$–400 °C with growth rate 1.0–5.0 nm s^{-1} on YbS buffer layers shows that lead chalcogenides grow as good-quality monocrystalline films despite the large lattice misfit:

Table 1
The crystal lattice period (a), melting temperature (T_{melt}) and bandgap E_g for the studied materials

	a (nm)	T_{melt} (°C)	$\alpha \cdot 10^{-6}$	E_g (eV)
PbSe	0.6122	1080	19,4	0.29
PbTe	0.6452	923	19,8	0.32
PbS	0.5935	1114	20,3	0.41
YbTe	0.6366	1730		0.95
YbSe	0.5879	2210	~19	2.00
EuSe	0.6188	2150	18,6	2.00
EuS	0.5970	2560	16	2.10
EuTe	0.6585	1525	18	2.20
YbS	0.5658	2130	18	1.70
Ge	0.56579	937	5,75	0.664
Si	0.5428	1688	2,4	1.09
BaF_2		~~1280~~	18,4	
KCl		~~357~~	37	

Table 2
The experimental X-ray rocking curve half-width ($\delta = 0.5 \times$ FWHM) and dislocation density (ρ) (calculated using Eq. (1)) for lead chalcogenide layers in the heterostructures studied

	δ (0.5 × FWHM, arcsec)	ρ (cm^{-2})
PbS/KCl	300	7×10^9
PbS–YbS/Si	200–300	$(3$–$7) \times 10^9$
PbSe–YbS/Si	100–200	$(0.8$–$3) \times 10^9$
PbTe–YbS/Si	200–300	$(3$–$7) \times 10^9$

PbS–YbS ($f = 4.8\%$), PbSe–YbS ($f = 7.9\%$), PbTe–YbS ($f = 13\%$).

Moreover, the quality of lead chalcogenide layers is better than for the YbS buffer layer. The XRRC half-widths for PbS ($\delta = 200$–300 arcsec), PbSe ($\delta = 100$–200 arcsec), and PbTe ($\delta = 200$–300 arcsec) layers are less than for the YbS buffer layer. If the XRRC half-width is due only to grown-in dislocations then we can estimate their density p [4] as

$$p = \delta^2 / 4.35 b^2 \quad (1)$$

where $b = a/2 < 110 >$ is the Burgers vector of edge dislocations (we used $b = 0.3$ nm as a value for an average b for lead chalcogenides), a is the lattice period, and δ is the X-ray rocking curve half width.

Table 2 shows that the quality of lead chalcogenide monocrystalline layers grown on (001) Si substrates with YbS buffer layers is no worse than for growth on (001) KCl. We can see, moreover, a substantial distinction between films on (001) KCl and (001) Si in the X-ray topography images (Fig. 1). X-ray topography shows that films on (001) KCl have monocrystalline blocks (owing to the substrate quality only) with typical dimensions ranging from 0.2 mm to 1.0 mm. However, the film grown on (001) Si has only one monocrystalline block, with the dimension of the substrate, without any grain boundaries present. This feature of IV–VI films on (001) Si is very important for integrated IR device manufacturing because it provides better homogeneity of electro-optical properties of the IR-sensitive layers.

Besides, the rare-earth chalcogenides are wide-gap semiconductors with good insulating properties and can therefore be used as insulator sublayers, very important for the formation of double-barrier tunnelling structures with resonant electron tunnelling, for example. In particular, the use of the wide-gap magnetic semiconductor EuS in combination with the conventional narrow-gap semiconductor PbS promises to create a new generation of electro-magneto-optical devices integrable with Si-based technology, with substantially different potential barrier heights for electrons with different spin directions (under conditions of field-induced magnetisation of EuS or by cooling below the Curie point [5]).

As for the use of YbS, it is the most promising material from the rare-earth chalcogenide family for buffer-layer growth on silicon substrates because it has the closest crystal lattice period to silicon (the lattice misfit with Si is $f = 4\%$)

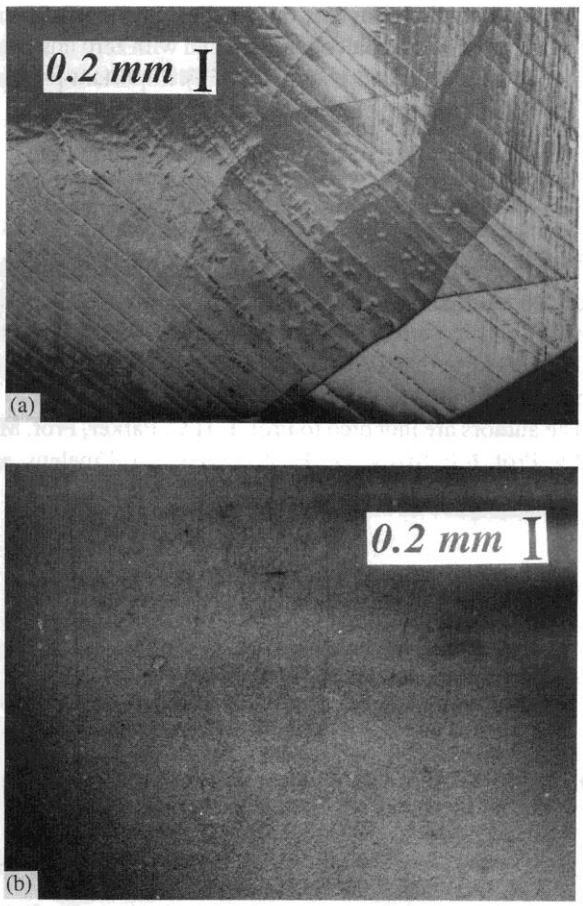

Fig. 1. X-ray topography images of (a) (001)PbS/KCl and (b) (001)PbS–YbS/Si heterostructures in the (311) reflection.

and in fact with zero mismatch to the Ge lattice parameter (see Table 1), a unique property for a new branch of Si–Ge technology [6,7].

3.2. Superlattices

X-ray diffraction patterns (Fig. 2(a)) show that YbS buffer layers allow the growth of IV–VI compound superlattices on (001) Si substrates with the same quality as on (001) KCl [6] but without block disorientation.

The lattice misfit f, period of misfit dislocations D, critical thickness of layers for misfit dislocation (MD) generation H_c, and minimum thickness of layers for superlattice formation H_m were determined for each pair of IV–VI and rare-earth chalcogenides (see Table 3).

In addition to fully strained SLs with pseudomorphic layer growth, it was found that one can create three-dimensional superlattices with periodic grids of MDs with composition modulation along the normal to SL plane (see Fig. 2(a) with satellite reflections S_n in the XRD patterns as a confirmation of such periodicity) and lateral periodicity owing to a dislocation strain modulation in its plane (see Fig. 2(b) with the plan-view TEM image). Such SL with MD [8,9] may be considered as a new kind of superlattice: we call it a misfit dislocation superlattice (MDSL).

The use of YbS buffer layers makes it possible to create the same (001) IV–VI MDSLs on (001)Si as on (001) KCl with three-dimensional (3D) periodic arrays of quantum dots and characteristic dimensions of confinement less than the distance between MDs, e.g. for PbSe–PbS SLs $D = 13.5$ nm, for PbSe–PbTe SLs $D = 8.4$ nm, and for PbTe–PbS SLs $D = 5.2$ nm. Previously, in comparison with PbSe-based 3D

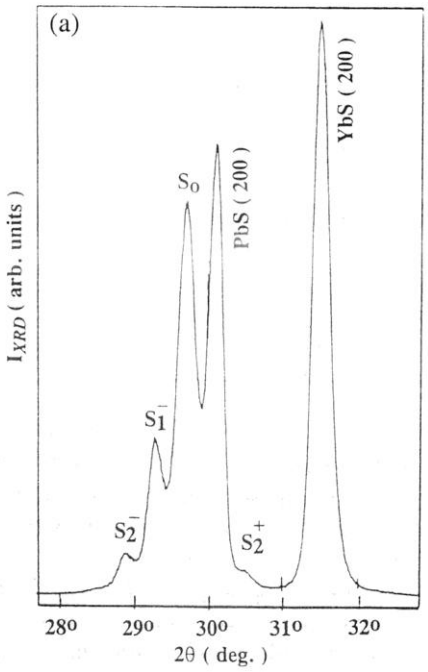

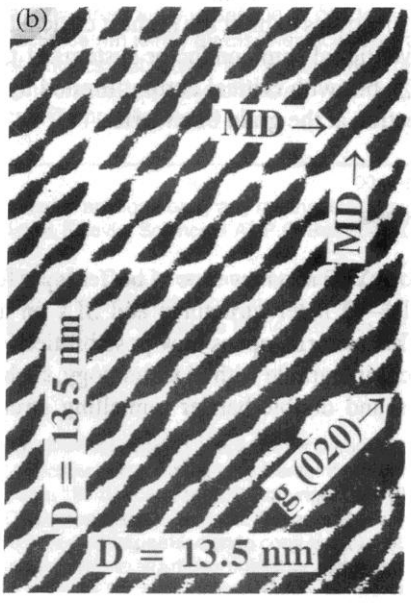

Fig. 2. (a) X-ray diffraction pattern for $(PbSe–PbS)_n$–YbS/(001) Si superlattice (sample 520) with period $D = 23.0$ nm ($D_{PbS} = 13.0$ nm and $D_{PbSe} = 10.0$ nm) and number of periods $n = 10$. Thicknesses of buffer layer YbS, 200 nm; and the first PbS layer, 150 nm. S_n, satellite reflections of the superlattice. (b) Plan-view electron-microscope image of the two-layer (001) PbSe–PbS structure with thicknesses of PbSe and PbS equal to 30 nm, where distance D between misfit dislocations (MD) equals 13.5 nm.

Table 3
Calculated (f and D) and experimentally measured (H_c, H_m) parameters for the studied superlattices

SL	f (%)	D (nm)	H_c (nm)	H_m (nm)
EuS–PbS	0.5	–	–	0.6
EuSe–PbSe	0.9	–	–	1.0
YbSe–PbS	0.9	–	–	1.0
PbTe–SnTe	2.1	23	10	1.4
EuS–PbSe	2.5	20	8	1.5
PbSe–PbS	3.1	13	6	1.5
SnTe–PbS	3.3	13	6	1.6
EuSe–PbS	4.0	12	6	1.8
YbSe–PbSe	4.1	10	5	2.0
EuSe–PbTe	4.4	10	4	2.0
YbS–PbS	4.8	8.5	3	2.0
PbTe–PbSe	5.3	8.4	3	2.0
EuTe–PbSe	7.2	6.2	2	3.0
EuS–PbTe	7.7	5.7	1	3.0
YbS–PbSe	7.9	5.2	1	3.5
PbTe–PbS	8.3	5.2	1	3.5
YbSe–PbTe	9.2	4.7	1	4.0
EuTe–PbS	10.0	4.3	1	4.0
YbS–PbTe	13	3.3	1	5.0

bulk and 2D systems [10], we have observed a large energy shift along with independence of temperature of the PL line position and width in the stimulated emission at temperatures of 5–90 K, as a quantum dot characteristic feature of (001) PbSe–PbS MDSLs [9].

The absence of block disorientation is very important for the future elimination of inter-block weak-link effects in the superconducting SLs (001) PbTe–PbS, which have unusual 2D high T_c-like superconductivity [11,12]. These SLs on (001) KCl substrates exhibit the highest critical temperature among conventional semiconductor systems at the moment ($T_c \leq 6.5$ K), but with critical current limited by poor electrical connection at the grain boundaries.

4. Conclusions

We propose YbS as a new type of buffer layer for epitaxial growth of IV–VI heterostructures and SLs on a (001) Si substrate. This material opens new possibilities for the creation of devices integrable with Si technology, such as IR focal plane arrays and double-barrier tunnelling structures. The buffer layer studied provides the smallest lattice misfit with Si (among rare-earth chalcogenides) and with zero mismatch to the Ge lattice parameter, a potentially important property for the development of Si–Ge technology [6,7].

Acknowledgements

This research has been supported in part by the Ukrainian State Committee on Science and Technology (Project Silicon-94) and in part by INTAS project 93-1403. One of the authors (OAM) thanks the Royal Society (UK) for financial support of his visit to Warwick University.

The authors are indebted to Prof. E.H.C. Parker, Prof. M.J. Kelly, Prof. F.F. Sizov, Dr. H. Zogg, Dr. C.J. Emeleus, and Dr. V. Tetyorkin for helpful discussions.

References

[1] H. Zogg, S. Blunier, T. Hoshino, C. Maissen, J. Masek and A. Tiwari, *IEEE Trans. Electron Dev., 38* (1991) 1110.
[2] I.V. Kolesnikov, V.A. Litvinov, A. Yu. Sipatov, A.I. Fedorenko and A.E. Yunovich, *Sov. Phys. JETP, 68*(1) (1988) 1431 [*Zh. Eksp. Teor. Fiz., 94* (1988) 239 (in Russian)].
[3] I.V. Kolesnikov and A. Yu. Sipatov, *Sov. Phys. Semicond., 23*(6) (1989) 598 [*Fiz. Tekh. Poluprovodn., 23*(6) (1989) 954 (in Russian)].
[4] L.S. Palatnik, *Structure and Physical Properties of Solids*, Vishaya Shkola, Kiev, 1983, p. 264 (in Russian).
[5] V.N. Lutskii, V.A. Petrov, A.S. Rylik, E.L. Galkin, A. Yu. Sipatov, A.I. Fedorenko and A.G. Fedorov, *Phys. Low-Dim. Struct., 7* (1994) 37.
[6] G. Abstreiter, *Solid State Commun., 92* (1994) 5.
[7] S.C. Jain and W. Hayes, *Semicond. Sci. Technol., 6* (1991) 547.
[8] L.S. Palatnik and A.I. Fedorenko, *J. Cryst. Growth, 52* (1981) 917.
[9] O.A. Mironov, A.I. Fedorenko, A. Yu. Sipatov, K.H. Herrmann and J.W. Tomm, *Abstract booklet of Int. Narrow Gap Semiconductors Conf.: NGS-95, Santa-Fe, USA, 8–12 January, 1995*, C13.
[10] K.H. Herrmann, J. Auth, KP. Mollmann, J.W. Tomm, H. Bottner, A. Lambrecht, M. Tacke, I.V. Kolesnikov, A.E. Yunovich, A.I. Fedorenko, O.A. Mironov and A. Yu. Sipatov, *Semicond. Sci. Technol., 8* (1993) S176.
[11] O.A. Mironov, V.V. Zorchenko, A. Yu. Sipatov, A.I. Fedorenko, O.N. Nashchekina and S.V. Chistyakov, *Defects and Diffusion Forum*, Scitec Publication LTD, Switzerland, Vols. 103–105, 1993, p. 473.
[12] O.A. Mironov, O.N. Makarovski, AI. Fedorenko, A.Yu. Sipatov, O.N. Nashchekina, I.M. Zaritskii and A.A. Konchits, *Acta Phys. Polon., A85* (1994) 603.